NASA/TM—1998-207941 AIAA–98–2599

Convective Instability of a Gravity Modulated Fluid Layer With Surface Tension Variation

J. Raymond Lee Skarda
Lewis Research Center, Cleveland, Ohio

Prepared for the
2nd Theoretical Fluid Mechanics Meeting
sponsored by the American Institute of Aeronautics and Astronautics
Albuquerque, New Mexico, June 15–18, 1998

National Aeronautics and
Space Administration

Lewis Research Center

June 1998

Available from

NASA Center for Aerospace Information
7121 Standard Drive
Hanover, MD 21076
Price Code: A03

National Technical Information Service
5287 Port Royal Road
Springfield, VA 22100
Price Code: A03

CONVECTIVE INSTABILITY OF A GRAVITY MODULATED FLUID LAYER WITH SURFACE TENSION VARIATION

J. Raymond Lee Skarda†
NASA Lewis Research Center, Cleveland, OH 44135

Abstract

Gravity modulation of an unbounded fluid layer with surface tension variations along its free surface is investigated. In parameter space of (wavenumber, Marangoni number) modulation has a destabilizing effect on the unmodulated neutral stability curve for large Prandtl number, Pr, and small modulation frequency, Ω, while a stabilizing effect is observed for small Pr and large Ω. As $\Omega \to \infty$, the modulated neutral stability curves approach the unmodulated neutral stability curve. At certain values of Pr and Ω multiple minima are observed and the neutral stability curves become highly distorted. Closed regions of subharmonic instability are also observed. Alternating regions of synchronous and subharmonic instability separated by very thin stable regions are observed in $(1/\Omega, g_1)$ space for the singly diffusive cases. Quasiperiodic behavior in addition to the synchronous and subharmonic responses are observed for the case of a double diffusive fluid layer. Minimum acceleration amplitudes were observed to closely correspond with a subharmonic response, $\lambda_{im} = \Omega / 2$.

1. Introduction

Under certain conditions such as thin liquid films or in a low-gravity environment, surface tension variations along a free surface may induce convection, referred to as thermocapillary convection. Orbiting spacecraft such as the NASA space shuttle and Russian Mir space station have proven to be useful environments for studying thermocapillary phenomena, which are often masked by gravity under terrestrial conditions. Thermocapillary phenomena are important to potential microgravity technologies such as crystal growing and materials processing applications as well as terrestrial applications such as coatings and drying processes. Onset of thermocapillary convection in the form of an extended Marangoni-Benard problem remains an active topic of study, in part due to its relative simplicity in terms of a motionless basic state and constant (or time periodic). The popularity of such models also stems from the understanding and insight they have provided to a broad range of physical phenomena (Pimputkar and Ostrach, 1981, Ostrach 1982, Davis 1987, Legro et. al, 1990, and Kochmeider 1993). Onboard space platforms the effects of vibration or g-jitter on thermocapillary systems is of particular concern (Nelson, 1991), although parametric excitation may also be of interest for terrestrial processes. With the question of g-jitter in mind, we focus on perhaps the simplest class of thermocapillary problems, the Marangoni-Benard problem, and consider how a fluid layer responds to time periodic accelerations or gravity modulation, which are imposed in the direction of the basic temperature gradient.

Gershuni and Zhukhovitskii (1963) and Venezian (1969) considered the effect of temperature modulation on the Rayleigh-Benard problems where buoyancy drives convection. Two papers, Gershuni, Zhukhovitskii, and Iurkov (1970) and Gresho and Sani (1970), address gravity modulation of the Rayleigh-Benard problem. Gershuni, Zhukhovitskii, and Iurkov (1970) considered the linear stability of an unbounded fluid layer and fluid with in a vertical circular cylinder with modulation of both the mean vertical temperature gradient and the vertical component of gravity, while Gresho and Sani (1970) studied both linear and nonlinear behavior of the gravity modulated unbounded layer. In both studies, a one-term Galerkin expansion reduced the equations to a single second order ordinary

† Research Engineer, Senior Member AIAA

differential equation, ODE. Applying a direct analogy to the viscously damped pendulum with an oscillating vertical support, Gresho and Sani (1970) recast the problem in terms of the Mathieu equation reducing the number of parameters affecting the system behavior from six (fluid transport) parameters to three (Mathieu) parameters. Murray et. al. (1991) and Wheeler et. al. (1991) treated the gravity modulated onset of convection problem with respect to directional solidification. In these papers it was shown that certain combinations of modulation amplitudes and modulation frequencies, stabilized the unmodulated fluid layer that would normally be unstable, or destabilized a fluid layer whose unmodulated state is stable.

More recently, Or and Kelly (1995) and Kelly and Or (1998) have investigated the effect of shear and temperature modulation on the Marangoni-Benard problem and noted interesting behavior that was also associated with surface deformation. For example, shear modulation by oscillating the lower (rigid) boundary destabilized the long wavelength mode but stabilized the finite wavelength modes. They found shear modulation could stabilize both finite and long wavelength modes while thermal modulation is effective in stabilizing the finite mode (Kelly and Or 1998).

The onset of convection (Rayleigh-Benard type) problem has been extended to double diffusive systems by Saunders et. al. (1992) and Terrones and Chen (1993). In these studies density gradients due to temperature and species concentration gradients drive convection. Terrones and Chen (1993) studied the linear stability of gravity modulation and cross-diffusion on the onset of convection in an unbounded doubly diffusive fluid layer. They considered the Soret and Dufour effects as well as cases where the cross-diffusion effects were directly imposed. The results of both Saunders et. al. (1992) and Terrones and Chen (1993) demonstrate a rich variety of behavior, such as synchronous, subharmonic, quasi-periodic, and multiple minima.

In this paper, parametric excitation of an unbounded fluid layer with surface tension variation along the free surface is considered and Floquet theory is applied to examine the stability of the modulated system. We initially focus on the gravity modulated Marangoni-Benard problem and then present a set of stability results for the modulated double diffusive Marangoni-Benard problem. The problem is first formulated for an unbounded double diffusive fluid layer where both density and surface tension variations due to temperature and/or concentration gradients induce convection.

2. Formulation of Equations and Boundary Conditions

An unbounded double diffusive fluid layer with dimension $0 \le x_3^* \le d$ is considered. The governing equations, continuity, momentum, energy, and species equations for incompressible flow are given below in Eqs. (1)-(4).

$$\frac{\partial U_i^*}{\partial x_i^*} = 0 \tag{1}$$

$$\frac{\partial U_i^*}{\partial t^*} + U_j^* \frac{\partial U_i^*}{\partial x_j^*} = \frac{-1}{\rho_o}\frac{\partial p^*}{\partial x_i^*} - \frac{\rho}{\rho_o} g_i^*(t^*)\delta_{i3} + \nu \frac{\partial^2 U_i^*}{\partial x_j^* \partial x_j^*} \tag{2}$$

$$\frac{\partial T^*}{\partial t^*} + U_j^* \frac{\partial T^*}{\partial x_j^*} = D_{11} \frac{\partial^2 T^*}{\partial x_j^* \partial x_j^*} \tag{3}$$

$$\frac{\partial c^*}{\partial t^*} + U_j^* \frac{\partial c^*}{\partial x_j^*} = D_{22} \frac{\partial c^*}{\partial x_j^* \partial x_j^*} \tag{4}$$

where δ_{ij} = Kronecker's delta and i=1,2,3 and * denotes dimensional quantities. The dependent variables U_i^*, T^*, and c^* are the velocity, temperature, and species, respectively. The time dependent body force term is periodic, of the form $g^*(t) = g_o^* + g_1^* \cos(\Omega^* t^*)$. Density, ρ, is computed using the Boussinesq approximation, $\rho = \rho_o\left\{1 - \beta_1\left(T^* - \overline{T}_0^*\right) - \beta_2\left(c^* - \overline{c}_0^*\right)\right\}$, where β_1 is the thermal expansion coefficient and β_2 is the solutal expansion coefficient. Reference values chosen for the buoyancy terms are the temperature and concentration basic state values of the lower surface, $\overline{T}_0^*$ and $\overline{c}_0^*$. The kinematic viscosity, ν, thermal diffusivity, D_{11}, and mass diffusivity, D_{22}, are assumed constant.

Impenetrable and no-slip velocity conditions are applied, and constant temperature and concentration are imposed at lower surface, $x_3^* = 0$.

At $x_3^* = 0$ (Bottom)

$$U_i^* = 0, \quad T^*(0) = \overline{T}_0^*, \quad c^*(0) = \overline{c}_0^*, \quad (\text{for } i = 1,2,3) \tag{6a-e}$$

The upper surface at $x_3^* = d$ is flat and nondeformable leading to equation (7a) while tangential stress balances

are given by(7b,c). Heat and mass flux conditions are given by equations (7d,e).

At $x_3^* = d$ (Top)

$$U_3^* = 0 \qquad (7a)$$

$$\mu\left(\frac{\partial U_3^*}{\partial x_j^*} + \frac{\partial U_j^*}{\partial x_3^*}\right) = -\gamma_1 \frac{\partial T^*}{\partial x_j^*} - \gamma_2 \frac{\partial c^*}{\partial x_j^*} \qquad (7a,b)$$

$$-\rho c_p D_{11} \frac{\partial T^*}{\partial x_3^*} = Q^*, \quad -D_{22} \frac{\partial c^*}{\partial x_3^*} = J^* \qquad (7d,e)$$

where: j = 1,2; and μ and c_p are the dynamic viscosity and specific heat, respectively, with constant values. Surface tension, σ, is approximated as a linearized function of the T^* and c^*, $\sigma = \sigma_0 - \gamma_1(T^* - \overline{T}_1^*) - \gamma_2(c^* - \overline{c}_1^*)$. The surface tension variation with temperature, γ_1, and the surface tension variation with concentration, γ_2, are defined as $\gamma_1 = -\left(\partial\sigma / \partial T^*\right)_{c^*,P^*}$ and $\gamma_2 = -\left(\partial\sigma / \partial c^*\right)_{T^*,P^*}$, respectively (Adamson 1982). Q^* and J^* are heat and mass fluxes to the environment at the free surface.

The velocity, temperature, and concentration basic state profiles are $\overline{U}^* = 0$,

$\overline{T}^*(x_3^*) = \overline{T}^*(0) - \Delta\overline{T}^* \frac{x_3}{d}$, $\overline{c}^*(x_3^*) = \overline{c}^*(0) - \Delta\overline{c}^* \frac{x_3}{d}$ where the difference quantities of the form Δy^* are defined as $\Delta y^* = y^*(0) - y^*(d)$. Following Joseph (1976), Saunders et. al. (1992), and Terrones and Chen (1993), the equations are linearized and then nondimensionalized. Reference values used to nondimensionalize the resulting disturbance equations are d, $\frac{D_{11}}{d}$, $\frac{d^2}{D_{11}}$, $\Delta\overline{T}^*$, $\Delta\overline{c}^*$ for length, velocity, time, temperature, and concentration, respectively. By assuming solutions of the form

$$(u(x_i,t), \theta(x_i,t), c(x_i,t)) = (w(x_3,t), \phi(x_3,t), \chi(x_3,t)) \exp(i(\alpha_1 x_1 + \alpha_2 x_2))$$

for the perturbation variables, velocity, u, temperature, θ, and concentration, c, the following disturbance equations of x_3-momentum, energy, and species are obtained.

$$\left(D^2 - \alpha^2\right)\dot{w} = -\Pr\alpha^2 g(t)\left(\mathrm{Ra}\,\phi + \mathrm{Rs}/\mathcal{D}_{22}\,\Theta\right) + \Pr\left(D^2 - \alpha^2\right)^2 w \qquad (8)$$

$$\dot{\phi} = \left(D^2 - \alpha^2\right)\phi + w \qquad (9)$$

$$\dot{\Theta} = \mathcal{D}_{22}\left(D^2 - \alpha^2\right)\Theta + w \qquad (10)$$

where $g(t) = g_o + g_1 \cos\Omega t$, $g_o = g_o^* / g_c$, $g_1 = g_1^* / g_c$, and $\Omega = \Omega^* D_{11} / d^2$.

Rigid, conductive, and permeable conditions, are imposed on the disturbance velocity, temperature and concentration at $x_3 = 0$. A flat-nondeforming free surface yields equation (12a) while the tangential stress balance is given by equation (12b). Equations (12c,d) are the disturbance flux conditions at the free surface.

$$\text{At } x_3 = 0, \quad w = 0 \quad Dw = 0 \quad \phi = 0 \quad \Theta = 0 \qquad (11a\text{-}d)$$

At $x_3 = 1$

$$w = 0 \qquad D^2 w = -\alpha^2\left(\mathrm{Ma}\,\phi + \mathrm{Ms}/\mathcal{D}_{22}\,\Theta\right) \qquad (12a,b)$$

$$D\phi + \mathrm{Nu}\,\phi = 0 \qquad D\Theta + \mathrm{Sh}\,\Theta = 0 \qquad (12c,d)$$

where D denotes $\partial / \partial x_3$ and $\dot{}$ denotes $\partial w / \partial t$. The resulting dimensionless parameters from the above equations are: the Prandtl number, $\Pr = \nu / D_{11}$, Diffusivity ratio, $\mathcal{D}_{22} = D_{22} / D_{11}$, thermal Rayleigh number, $\mathrm{Ra} = g_c \beta_1 \Delta\overline{T}^* d^3 / D_{11}\nu$, solutal Rayleigh number $\mathrm{Rs} = g_c \beta_2 \Delta\overline{c}^* d^3 / D_{22}\nu$, thermal Marangoni number, $\mathrm{Ma} = \gamma_1 \Delta\overline{T}^* d / D_{11}\mu$, solutal Marangoni number, $\mathrm{Ms} = \gamma_2 \Delta\overline{c}^* d / D_{22}\mu$, surface Nusselt number, $\mathrm{Nu} = h_1 d / \kappa$, surface Sherwood number, $\mathrm{Sh} = h_2 d / D_{22}$.‡

The disturbance equations are reduced to a set of N ordinary differential equations, ODE's, using a spectral (Chebyshev) collocation scheme. Floquet analysis is applied to examine the stability of the system of ODE's (Meirovitch 1970, and Joseph 1976). The monodromy matrix is computed by integrating the N set of ODE's N times. Floquet multipliers, ρ_j, which are the eigenvalues of the monodromy matrix are then computed, and the characteristic exponents, λ_j, which determine the stability of the system are related to the floquet multipliers as $\lambda_j = \frac{1}{T}\ln(\rho_j)$. The characteristic exponent with the largest real part, λ, determines the stability of the system. If Re(λ) is positive, disturbances grow, if Re(λ) is negative, disturbances decay. The imaginary part of λ is multivalued and characterizes the

‡ h_1 and h_2 are surface heat and mass transfer coefficients defined in Pearson 1958, and Skarda et. al. 1998 (among several refs.). κ is the thermal conductivity of the fluid layer.

system response. The response is synchronous when $\mathrm{Im}(\lambda) = n\Omega$, and subharmonic when $\mathrm{Im}(\lambda) = \left(n + \frac{1}{2}\right)\Omega$, where n is an integer value. When the two frequencies are incommensurate, $|\delta| \neq n$ for $\mathrm{Im}(\lambda) = \delta\frac{\Omega}{2}$, the response is quasiperiodic (Joseph 1976, Saunders et. al. 1992, and Terrones and Chen 1993).

3. Results For Modulated Singly Diffusive Fluid Layer

The effect of modulation frequency on neutral stability is first examined in (α,Ma) space, typically used to study stability behavior of the unmodulated Marangoni-Benard problem. The set of neutral stability curves in Figs. 1a-f corresponds to Pr, g_1, and Ra values of 1, 5 and 1000, respectively. Below each curve, the system is stable and "small" disturbances decay, and above the curve, the system is unstable and the disturbances will grow in time. The unmodulated neutral stability curve is shown in each figure as a reference point to directly compare and contrast the effect of modulation on the neutral stability boundaries.

Fig. 1a reveals the existence of two small local minima (denoted as humps) near the bottom of the neutral stability for Ω=7. Ma_c is associated with hump 3 in Fig. 1a and shifts to hump 2 for Ω=10 indicated in Fig. 1b. This suggests that a double minima exists along the synchronous curve for some Ω between 7 and 10. In Fig. 1c where Ω =14.5, hump 2 forms a narrow finger that extends below the unmodulated Ma_c of 80, thus having a destabilizing effect on the unmodulated neutral stability curve. Another local minimum, hump 1, is found near α=1 in Fig. 1c. Examination of Figs. 1d-f indicates hump 1 continues to grow as hump 2 recedes with increasing Ω, suggesting the presence of another double minima. Hump 2 eventually disappears with increasing modulation frequency. Between Ω of 17 and 18, a subharmonic closed neutral stability branch forms. The subharmonic region of instability grows with increasing modulation frequency until reaching an Ω of approximately 35. The subharmonic branch then begins to shrink and shifts to higher wavenumbers and lower Marangoni numbers. The subharmonic branch continues to shrink and eventually disappears as Ω increases to a value of 100 where only the synchronous branch is evident. For $\Omega \geq 100$ the subharmonic loop

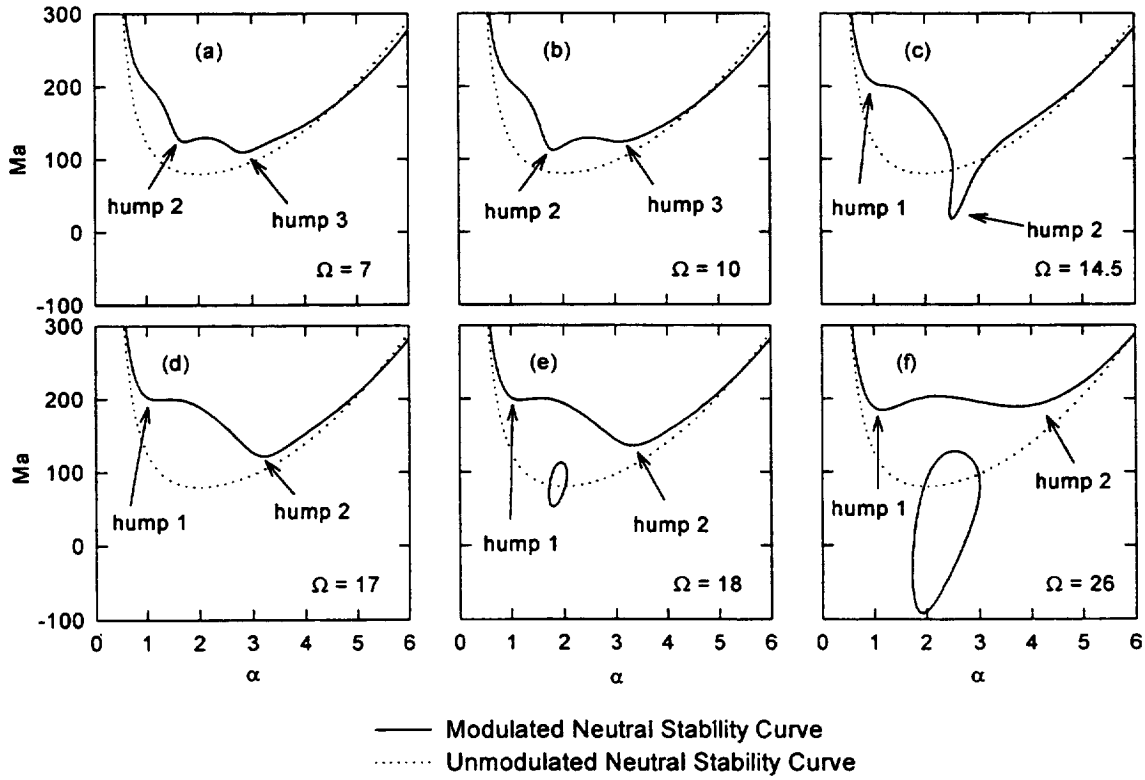

Figure 1 Neutral Stability Curves for Pr=1., g_0=0, g_1=5, Ra=1000

shifts out of the range of Ma values explored while modulation is observed to have a stabilizing effect on the synchronous branch. The stabilization effect however diminishes with further increase of the modulation frequency. The shapes of the neutral stability curves also change with modulation.

The behavior of critical Marangoni numbers, Ma_c, and critical wavenumbers, α_c, with respect to modulation frequency are shown in Figs. 2 through 3 for Pr values of .01, 7.1, 10 and 100. In view of the complex topology of the neutral stability curves, the critical values for Pr=1 are presented separately in Figs. 4 and 5. This level of complexity was not observed in the neutral stability plots at the other Pr values (for the range of parameter values we investigated) therefore we discuss these Pr values first.

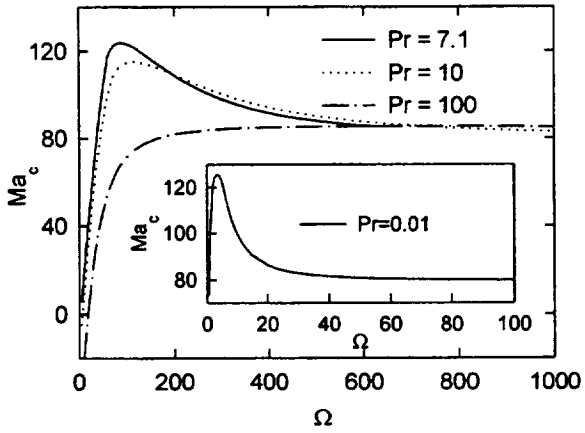

Figure 2 Critical Ma_c versus modulation frequency, Ω, for varying Pr values. Ra = -1000, $g_0 = 0$, $g_1 = 5$.

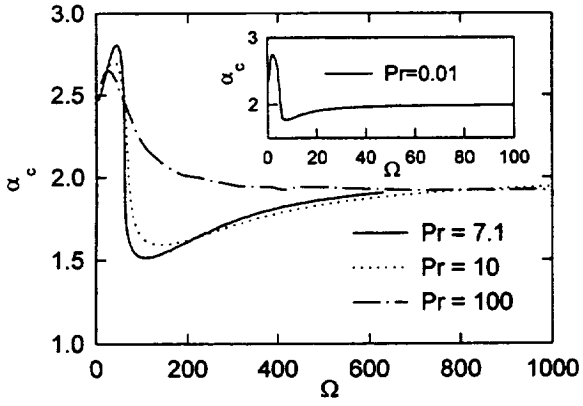

Figure 3 Critical wavenumber, α_c, versus modulation frequency, Ω, for varying Pr values. Ra = -1000, $g_0 = 0$, $g_1 = 5$.

Gravity modulation for sufficiently small Ω, is destabilizing for all Pr values investigated. As Ω increases, gravity modulation has a stabilizing effect on Ma_c which reaches a maximum at some finite values of Ω. The stabilizing effect then decreases with a further increase in Ω, and approaches the unmodulated critical value of Ma_c=79.607 as $\Omega \to \infty$. Values of Ma_c, Ω, and α_c where maximum stabilization occurs are given in Table 1.

Table 1 Values of Ω, Ma_c, and α_c for maximum stabilization

Pr	g_1	Ω	Ma_c	α_c
.01	5	3.4	125.77	2.68
7.10	5	88.0	123.67	1.54
10.00	5	116.0	115.20	1.60
100.00*	5	1000.0*	85.09*	1.92*

* Maximum Stabilization Occurs Beyond Ω=1000

Critical and extremum values of Ma and α for Pr=1 are shown in Figs. 4 and 5. Critical Marangoni numbers and wavenumbers of the synchronous branch are shown as functions of modulation frequency in Figs. 4a,b, while extremum values of Ma_C and α_C for the subharmonic branch are shown in Figs. 5a,b.

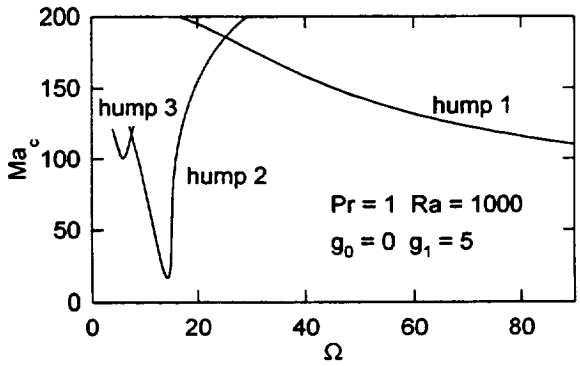

Figure 4a Ma_C versus Ω for the synchronous branch. For Pr=1

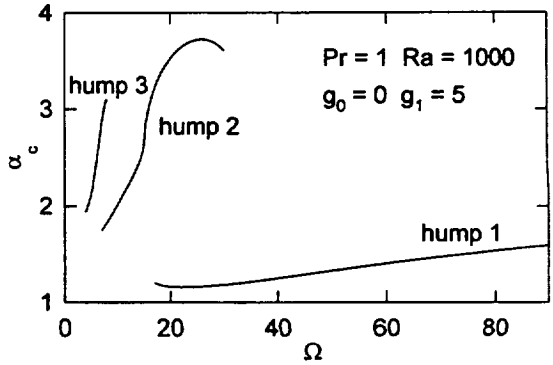

Figure 4b α_C versus Ω for the synchronous branch. For Pr=1

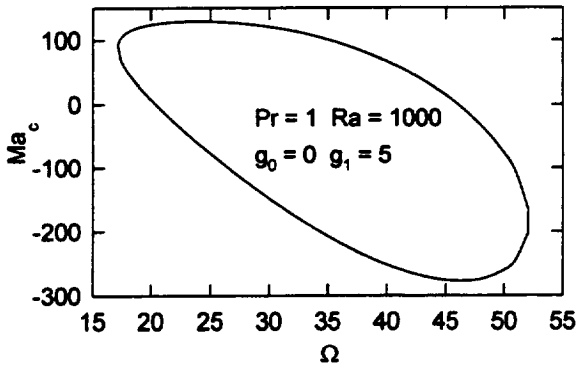

Figure 5a Ma_c versus Ω for the subharmonic branch. For Pr=1

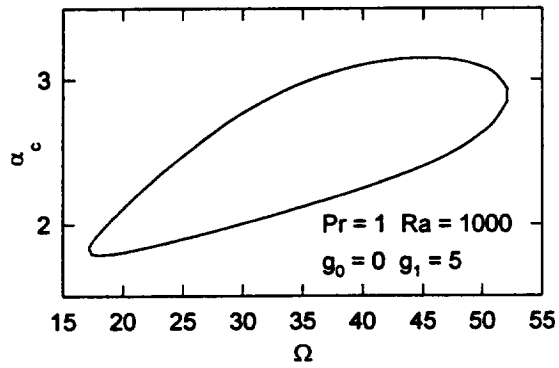

Figure 5b α_c versus Ω for the subharmonic branch. For Pr=1

The location and critical values corresponding to the two double minima observed in Fig. 4a are given in Table 2. Physically, the double minima suggest possible occurrence of mode switching where the cellular (or roll) pattern alternates between two cell or roll sizes dictated by the two different wavenumbers. Such a process would be easily observed given the large difference in the two wavenumbers associated with each of the double minima in Table 2.

Table 2 Location and critical values for double minima

Ω	Ma_c	α_{c1}	α_{c2}
9.00	124.0	1.7	3.1
25.24	185.7	1.2	3.5

Figs. 5a,b reveal that the subharmonic branch forms at an Ω slightly less than 17.5 and disappears just beyond an Ω of 52. The subharmonic instability extends to Ma values less than -250, where stable temperature gradient occurs for the unmodulated problem.

3.2 Modulated Marangoni-Benard & Rayleigh-Benard Instabilities in $(1/\Omega,g_1)$ Space

For the unmodulated problem, neutral stability curves in (α,Ma) space for the Marangoni-Benard problem are qualitatively similar to those of the Rayleigh-Benard. Unfortunately this correspondence of stability behavior between (α,Ma) space and (α,Ra) space does not hold for the modulated problem. This is because changing Ra simultaneously effects both the steady instability agency (buoyancy) and the modulation amplitude which is also part of the buoyancy term. In contrast, varying Ma only effects a steady instability agency - that of the surface tension variation. The result is that stability behavior observed in the (α,Ra) plane is not likely to apply to similar conditions in the (α,Ma) plane. A more appropriate space to compare the modulated Rayleigh-Benard and Marangoni stability behavior is that of $(1/\Omega,g_1)$ space.

Three neutral stability maps in $(1/\Omega,g_1)$ space corresponding to different values of Ma, and g_0 are shown in Figs. 6a,b,c. The values of α, Ra, and Pr are 2, 1000, and 1, respectively, for these figures. For g_0= 1, the Rayleigh number of 1000 in Fig. 6a, is 49.2% higher than the unmodulated neutral stability Rayleigh number at α=2. In Fig. 6b, the mean gravity acceleration level, g_o, and Ma are zero: therefore both the steady instability agencies of buoyancy and surface tension are zero. And in Fig. 6c, the Marangoni number is 118.77, which is 49.2% greater than the unmodulated neutral value of Ma at α=2.

Results in Fig. 6a correspond to the modulated Rayleigh-Benard problem with a rigid-conductive lower surface and a free-insulated upper surface while the steady gravity acceleration level, g_0, is set to one which corresponds to terrestrial conditions. Fig. 6a reveals that a finite acceleration amplitude is required to stabilize the layer. Further increase in g_1 eventually destabilizes the layer. In general, alternating bands of synchronous and subharmonic instability separated by thin stable regions are observed in Fig 6a which is also characteristic of temperature modulation results of Gershuni and Zhukhovitskii (1963) and Kelly and Or (1998). Gershuni and Zhukhovitskii (1963) referred to the lower most region of instability as the fundamental instability region and showed that it existed for Ra values exceeding the unmodulated neutral Ra value[§].

[§]The situation equally applies to the Marangoni-Benard problem where Ma values replaces Ra values.

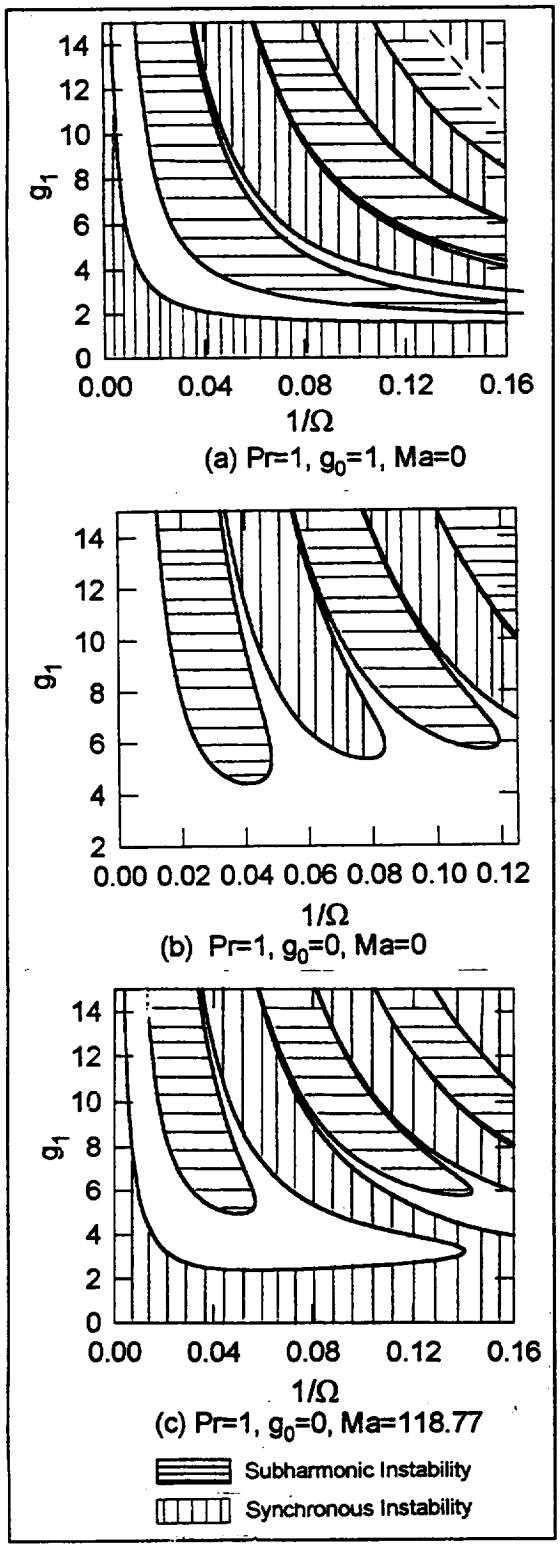

Figures 6a, b, c. Stability boundaries in $(1/\Omega, g_1)$ space for α=2 and Ra=1000.

In Fig 6b, the steady acceleration level is $g_o = 0$, corresponding to a zero gravity condition while all other parameter values and boundary conditions are identical those applied in Fig. 6a. Since mean instability agencies are zero for these results, i.e., Ma=g_0=0, no fundamental instability exists. The system is stable for all frequencies until a finite amplitude value is reached. The stable regions separating the fingers of instability become quite thin with decreasing frequency and increasing modulation amplitude. A similar set of results, but with free-conductive boundaries was presented by Saunders et al. (1992). They chose Ra and Pr values of 1000 and .1, respectively, and $\alpha = \pi/2$. While their Pr and wavenumber differ from the Pr and α values used for Fig. 6, the shape and orientation of the instability fingers are quite similar. Their minimum modulation amplitude for instability was 7.3 corresponding to an Ω of 10.5 as compared to the minimum amplitude of 4.05 and Ω of 24.4 for Fig. 6b.**

The gravity modulated Marangoni instability shown in Figs. 6c, exhibits a fundamental instability band for small values of g_1. This is consistent with the Rayleigh-Benard instability discussed for Fig. 6a, since Ma exceeds its corresponding unmodulated neutral stability value, Ma=79.6. A minimum finite amplitude of 4.97 is reached at Ω=20.0 where modulation stabilizes the fundamental instability. At larger amplitude, the resonant instability regions or fingers, are attained as in Fig. 6b. The appearance of the synchronous and subharmonic instability regions is qualitatively different from the modulated Rayleigh-Benard problem observed in Fig. 6a. In Fig. 6c, multiple regions of stability exist that engulf each of the subharmonic instability fingers, and a single region of synchronous instability, the fundamental instability, surrounds the multiple stable regions. In all plots in Fig. 6a,b,c, regions of alternating subharmonic/synchronous instability occur and are separated by regions of stability.

4.0 Results For The Double Diffusive Fluid Layer

The large parameter space associated with the gravity-modulated doubly-diffusive Marangoni instability problem poses a serious challenge to a full characterization of such systems. For our doubly diffusive gravity-modulated problem there are twelve parameters (Pr, Ra, Rs, Ma, Ms, α, Nu, Sh, D_{22}, g_o, g_1,

** For consistency, Saunders et al.'s (1992) dimensionless frequency was converted to Ω defined herein by $\Omega = \mathrm{Pr}\,\Omega_{\text{Saunders}}$.

Ω).[††] The difficulty in handling large parameter spaces was similarly acknowledged in the gravity modulated Rayleigh-Benard investigations of Saunders et. al. (1992) and Terrones and Chen (1993). For this study, we choose a single set of values for (Pr, $\mathcal{D}_{22}$, Ra, Rs, Ms, Nu, Sh, g_o), and again investigate stability behavior in the parameter spaces of (α,Ma) and ($1/\Omega$,g_1).

4.1 Stability Boundaries For Unmodulated Double Diffusive System

For the unmodulated double diffusive problem, oscillatory (diffusive) neutral stability associated with a Hopf bifurcation is possible, in addition to the stationary (fingering) instability resulting from an exchange-of-stabilities that typically occurs for the singly unmodulated Benard problem. Modulated behavior also differs depending on the nature of the unmodulated instability, oscillatory or stationary. Therefore, we first compute stability boundaries for the unmodulated double diffusive problem using a normal mode analysis and use these results to choose parameter values that yield the desired behavior i.e. stationary or oscillatory.

Stability boundaries are shown in (Ms_c,Ma_c) space in Fig. 7 for the parameter set (Pr,$\mathcal{D}_{22}$,Ra,Rs,Nu, Sh) with values (10,0.1,500,-500,0,0). The Pr value is representative of water-alcohol or thermohaline systems, although, $\mathcal{D}_{22}$ for such systems is normally in the range, 10^{-3} to 10^{-2}. The shape of the stability boundaries is also characteristic of double diffusive systems with the small $\mathcal{D}_{22}$ values (Legros 1990, Terrones & Chen 1993, Skarda et. al. 1998). A co-dimension two point, represented by the intersection of the oscillatory and stationary boundaries occurs at the point, (Ms_c,Ma_c) = (-9.0, 88.6). To the left of the co-dimension two point, the transition from stable to unstable behavior occurs via a Hopf bifurcation and oscillatory neutral stability behavior is observed. To the right of the co-dimension two point exchange of stability is observed resulting in the presence of stationary neutral stability boundary. Frequencies, λ_{im}, and critical wavenumbers, α_c, associated with the oscillatory stability boundary are shown in the insert of Fig. 7. (Here, λ is the eigenvalue with the largest real part obtained from a normal mode analysis of the unmodulated problem (Pearson 1958, Joseph 1976, Skarda et. al. 1998)). Both λ_{im} and α_c increase with increasing Ma_c values, moving to the left of and away from the co-dimension two point.

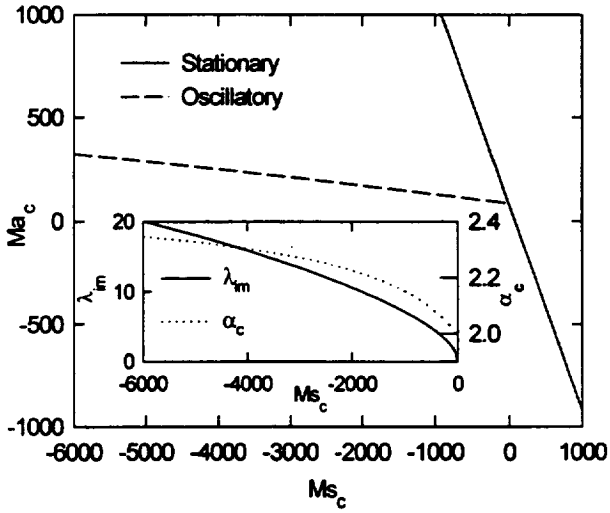

Figure 7 Stability Envelope for Pr=10, D_{22}=0.1
(Insert shows variation of frequency, λ_{im}, and wavenumber, α_c)

4.2 Gravity Modulated Double Diffusive Layer

For the parameter values we chose that correspond to the stationary (fingering) instability, $\lambda_{im} = 0$, the modulated stability behavior is similar to the singly diffusive results discussed in the previous section. However, for parameter values corresponding to oscillatory (diffusive) behavior, $\lambda_{im} \neq 0$, of the unmodulated system, a rich variety of behavior is possible along the neutral stability curve. Only results for parameter values corresponding to oscillatory behavior are presented below.

The effect of frequency modulation on neutral stability curves is shown in Figs. 8a, and 8b. The elements of the parameter set (Pr, $\mathcal{D}_{22}$, Ms, Ra, Rs, Nu, Sh, g_0) are chosen as (10, 0.1, -700, 1000, -1000, 0, 0, 0), which correspond to oscillatory neutral stability behavior of the unmodulated problem. The unmodulated double diffusive neutral stability curve is provided in Figs. 8 for comparison with modulated curves, and is represented by the dotted line. The corresponding frequency, λ_{im}, values are shown in Figs.9a and 9b. The locations of the bifurcation points along the modulated neutral stability curves are tabulated in Table 3. Quasiperiodic behavior occurs when λ_{im} and Ω are incommensurate. For the oscillatory region of the unmodulated layer, oscillatory behavior occurs, while a complicated temporal flow structure occurs for the quasiperiodic region of the modulated fluid layer in Figs. 8a and 8b.

[††] Even the singly-diffusive gravity-modulated problem required consideration of eight parameters.

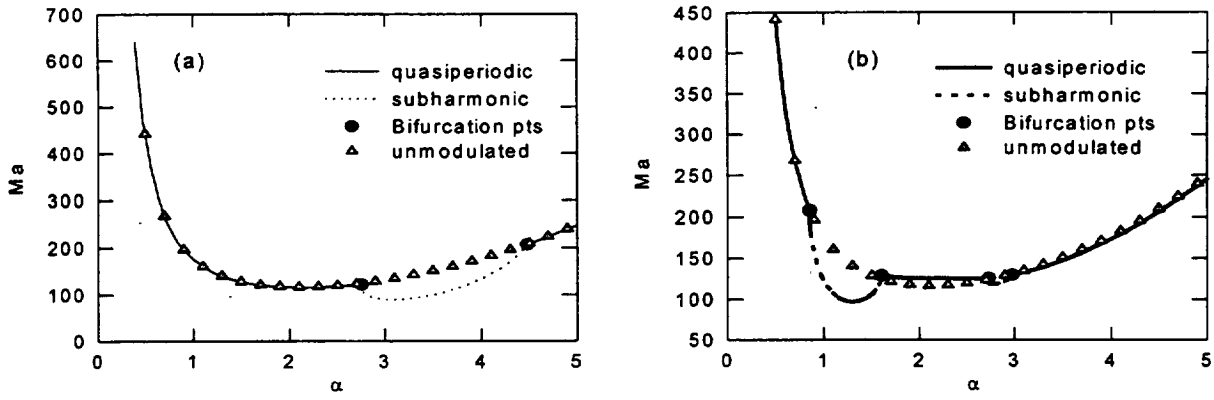

Figure 8. Neutral Stability curves for gravity modulated doubly diffusion. Ms = -700, Pr = 10, $\mathcal{D}_{22}$ = 0.1, Ra = 1000, Rs = -1000, g_0 = 0, g_1 = 1. (a) Ω=20, (b) Ω=5.

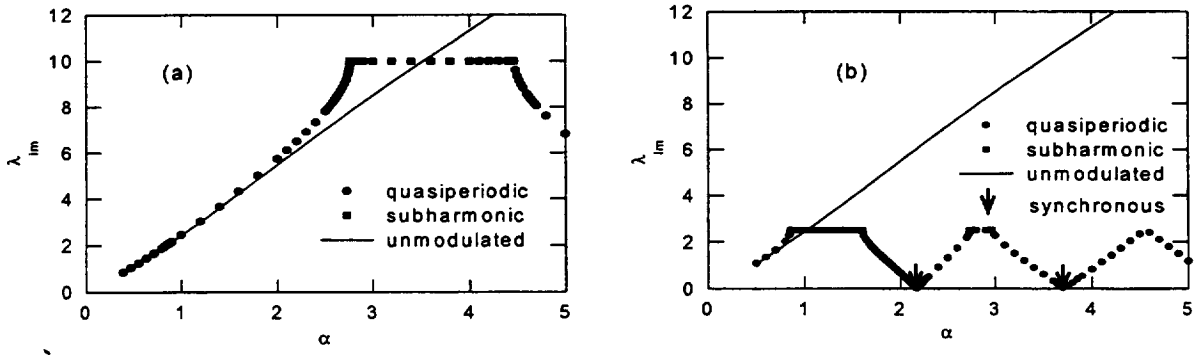

Figure 9 Imaginary part of most unstable characteristic root, λ_{im}. Parameters, Ms, Pr, $\mathcal{D}_{22}$, Ra, Rs, g_0, and g_1, have same values as those used for figure 8. (a) Ω = 20, (b) Ω = 5.

Table 3 Location of Bifurcation Points For Neutral Stability Curves in (α,Ma) space Pr=10 $\mathcal{D}_{22}$=.1 Ra=500 Ms=-700 Rs=-500 g_0=0 g_1=1

Ω	Bifurc Type	α_{bifr}	Ma_{bifr}	$\lambda_{im\ bifr}$
20	qu → sub	2.76	122.5	10.0
	sub → qu	4.48	206.8	10.0
5	qu → sub	0.86	208.0	2.5
	sub → qu	1.61	129.0	2.5
	qu – syn – qu	2.18	125.7	5.0
	qu → sub	2.74	126.1	7.5
	sub → qu	2.98	129.5	7.5
	qu – syn – qu	3.71	157.0	10.0

* Subharmonic loop also observed for Ω=50

Two bifurcation points are observed along the doubly diffusive stability curve for Ω=20 shown in Fig. 8a. Moving from left to right along the neutral stability curve, quasiperiodic behavior gives way to subharmonic behavior which in turn bifurcates to quasiperiodic behavior again. Values of α and Ma corresponding to the bifurcation points are given in Table 3. The critical Marangoni number, Ma_c, occurs in the subharmonic region. However, careful examination of Fig. 8a also reveals the existence of a local quasiperiodic minimum.

Reducing the modulation frequency further to Ω=5 increases the complexity of behavior along the neutral stability curve. Six bifurcation points are shown in Fig. 8b. Five regions of quasiperiodic behavior are separated by intervals or points of subharmonic, synchronous, subharmonic, and synchronous behavior, respectively. The critical Marangoni number, Ma_c is subharmonic, with local minima occurring in quasiperiodic and other subharmonic regions as well. Values of α, Ma, and λ_{im}, corresponding to the bifurcation points are given in Table 3.

The frequency, λ_{im}, plots in Figs. 9a and 9b confirm that resonance is responsible for the bifurcations observed in Figs. 8a and 8b. Resonant behavior is expected when λ_{im} and Ω are commensurate, i.e., $\lambda_{im} = \frac{n\Omega}{2}$, where n is an integer

value. The maximum value of λ_{im} over the range $0.5 \le \alpha \le 5$ for the unmodulated layer is 14.06, therefore, resonance is anticipated at some location along the neutral stability curve where the modulation frequency, Ω, satisfies $\Omega \le 28.12$. Subharmonic excitation is clearly visible in Figs. 9a and 9b as λ_{im} approaches the $\frac{\Omega}{2}$ value of 10 and 2.5 respectively. The smallest wavenumber, α, where λ_{im}=5 in Fig. 9a is 2.76, which is a quasiperiodic to subharmonic bifurcation point given in Table 3. Similar behavior occurs in Fig. 9b for λ_{im}=2.5. For Ω= 5, both subharmonic and synchronous resonances occur for α values where the unmodulated λ_{im} of 2.5, 5, 7.5, 10 are obtained.

The doubly diffusive Marangoni instability was also investigated in $(1/\Omega, g_1)$ space for a set of parameter values where unmodulated oscillatory behavior occurs. Values of α and Ma were chosen as 2.2 and 111, respectively, while other parameters maintain their values prescribed above. This parameter set yields an oscillatory and slightly stable behavior in the absence of modulation where the eigenvalue with the largest growth rate was computed as λ = - 0.2422 + i 6.137.

The stability boundaries in $(1/\Omega, g_1)$ space are shown in Fig. 10. A single continuous region of subharmonic instability was observed for sufficiently large modulation amplitudes, g_1. The subharmonic instability region extends to small g_1 values on either side of a small closed loop region of synchronous instability. A minimum amplitude, g_1=0.228 is necessary to destabilize the layer. The parametric response, $\frac{n\Omega}{2}$, in this case is subharmonic, where the corresponding modulation frequency is Ω=12.3 which is twice the value of the unmodulated λ_{im} indicated above. Quasiperiodic behavior was observed for Ω>19.05.

Time histories for the velocity, temperature, and species disturbances of a double diffusive fluid layer are shown in Figs. 11-13. Parameter values for all three cases correspond to neutrally stable systems. Oscillatory behavior for an unmodulated fluid layer is shown in Figs. 11 The subharmonic and quasiperiodic behavior shown in Figs. 12 and 13 correspond to parameter values chosen at two different locations along the neutral stability curve in Fig. 8b.

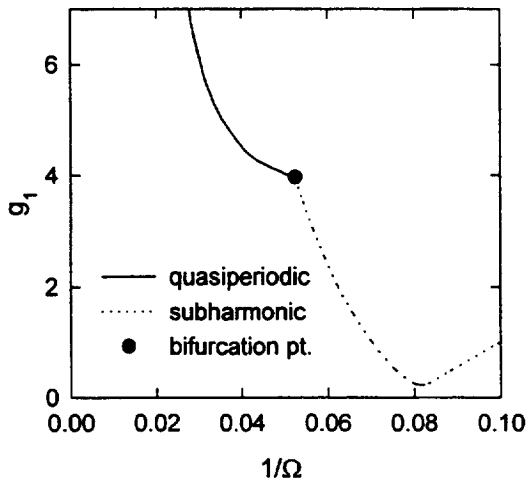

Figure 10. Modulated double-diffusive Marangoni-Benard stability boundaries in $(g_1, 1/\Omega)$ space. α = 2.2, g_o = 0, Pr = 10, $\mathcal{D}_{22}$ = 0.1, Ra = 500, Rs = -500, Ma = 111, Ms = -700.

5. Conclusions

The stability behavior for both the singly and doubly diffusive Marangoni-Benard problems is more complex in the presence of modulation. For the singly diffusive problem, modulation had a stabilizing effect on neutral stability curves in (α,Ma) space at large modulation frequencies and approached the unmodulated neutral stability curve as $\Omega \to \infty$. For a Pr of 1, both synchronous and subharmonic regions of instability were observed for certain values of modulation frequency. The synchronous branch became distorted with local minima and narrow fingers forming at certain values of Ω. Sometimes both local minima were above the unmodulated Ma_c, thus resulting in a stabilizing effect. At other times one local minimum extended below the unmodulated Ma_c. Maximum stabilization, (largest Ma_c) occurred at some finite value of modulation frequency.

In previous modulated Rayleigh-Benard studies, alternating regions of harmonic and subharmonic were observed in $(1/\Omega, g_1)$, however the shape of the unstable regions from those of the present modulated Marangoni study qualitatively differed. For the Marangoni-Benard problem, multiple regions of stability exist that engulf each of the subharmonic instability fingers, and a single region of synchronous instability, the fundamental instability, surrounds the multiple stable regions.

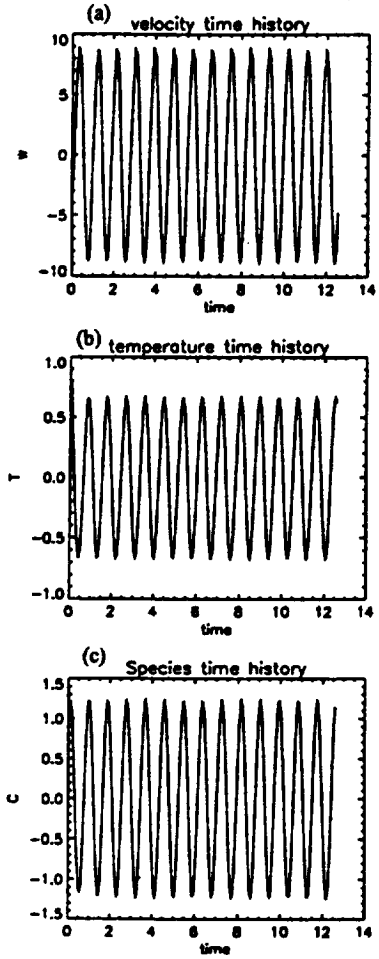

Figure 11 unmodulated oscillatory behavior

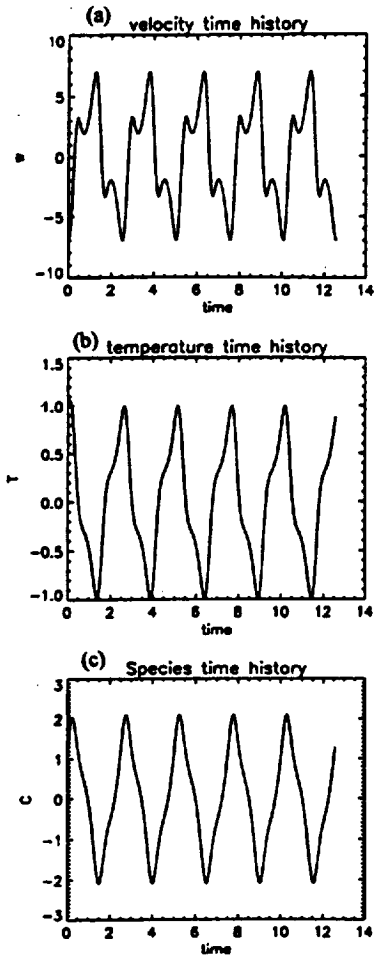

Figure 12 subharmonic behavior

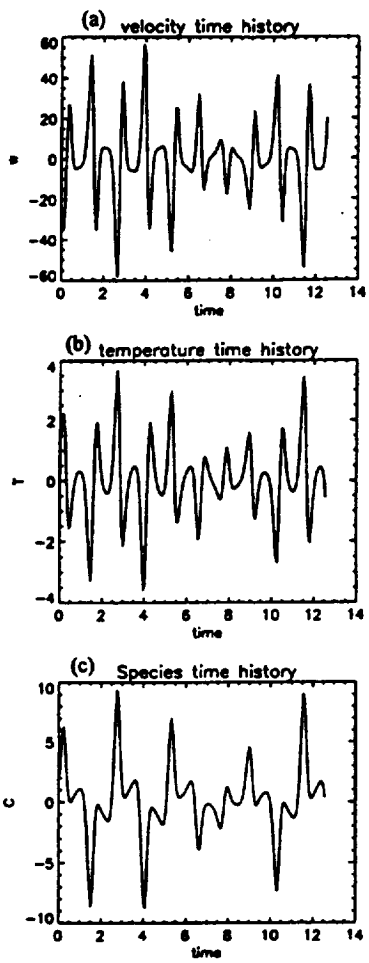

Figure 13 quasiperiodic behavior

Figures 11-13. Time histories of velocity, temperature, and species disturbances at the center of the layer, z=0.5, for neutral stability. Pr = 10, $\mathcal{D}_{22}$ = 0.1, Ms = -700, Ra = 1000, Rs = -1000, g_o = 0, Ω = 5. Figure 11, α = 2.5, Ma = 119.86. Figure 12, α = 1.2, Ma = 99.2777., Figure 13, α = 2.7, Ma = 125.8057.

The gravity modulated doubly diffusive Marangoni instability was considered for a single set of Pr and $\mathcal{D}_{22}$ values. For parameter values corresponding to the stationary (fingering) instability, the modulated behavior is similar to the singly diffusive results. When parameter values correspond to oscillatory (diffusive) behavior, $\lambda_{im} \neq 0$, of the unmodulated system, regions of quasiperiodic, subharmonic and synchronous behavior were found to exist along the neutral stability curves. This behavior is consistent with that of the double diffusive Rayleigh-Benard instability reported by Saunders et. al. (1992) and Terrones and Chen (1993). As modulation frequency, Ω, was decreased, bifurcations along the neutral stability curve became more frequent due to parametric resonances. For a given value of λ_{im}, accompanied by a decrease in Ω, clearly the number of bifurcations increases as $n = \frac{\lambda_{im}}{2\Omega}$ (n is an integer value only). In $(1/\Omega, g_1)$ space, the minimum g_1 necessary to destabilize the layer was the result of subharmonic excitation and thus occurred at a modulation frequency twice the value of the unmodulated λ_{im}.

References

Adamson, A.W. 1982 *Physical Chemistry of Surfaces*, 4th edn. John Wiley.

Davis, S.H. 1987, "Thermocapillary Instabilities," Annual Review of Fluid Mechanics, Vol. 19, pp. 403-435.

Gershuni, G.Z. and E.M. Zhukhovitskii, 1963, "On Parametric Excitation of Convective Instability," PMM., Vol. 27, No. 5, pp. 779-783.

Gershuni, G.Z., E.M. Zhukhovitskii, and I.S. Iurkov, 1970, "On Convective Stability In the Presence of Periodically Varying Parameter," Journal of Applied Math. Mech., Vol. 34, pp. 442-452.

Gresho, P.M., and R.L. Sani, 1970, "The Effects of Gravity Modulation on the Stability of a Heated Fluid Layer," Journal of Fluid Mechanics, Vol. 40, No. 4, pp. 783-806.

Joseph, D.D., 1976, *Stability of Fluid Motions*, Springer-Verlag, New York.

Kelly, R.E., and Or, A.C., 1998, " Influence of Temperature Modulation Upon The Onset of Thermocapillary Convection," 36th Aerospace Sciences Meeting, Reno, NV, AIAA 98-0652.

Koschmieder, E.L., 1993, *Benard Cells and Taylor Vorticies*, Cambridge University Press.

Legros, J.C., Dupont, O., Queeckers, P. Van Vaerenberg, S., 1990, "Double-Diffusive Convection And Its Effect Under Reduced Gravity," *In Low Gravity Fluid Dynamics and Transport Phenomena*, ed. Koster, J.N. and R.L. Sani, American Institute of Aeronautics and Astronautics, Washington D.C.

Meirovitch, L., 1970, *Methods of Analytical Dynamics*, McGraw-Hill Book Co. N.Y.

Murry, B.T., S.R. Coriell, and G.B. Mcfadden, 1991, "The Effect of Gravity Modulation On Solutal Convection During Directional Solidification," Journal of Crystal Growth, Vol. 110, pp.713-723.

Nelson, E.S., 1991, "An Examination of Anticipation of g-jitter on Space Station and Its Effects on Material Processes, NASA TM 103775.

Or, A.C. and Kelly, R.E., 1995, "Onset of Marangoni Convection in a Layer of Fluid Modulated by Weak Nonplanar Oscillatory Shear," International Journal of Heat and Mass Transfer, Vol. 38, No. 12, pp. 2269-2279.

Ostrach, S., "Low-Gravity Fluid Flows," Annual Review of Fluid Mechanics, Vol. 14, 1982, pp. 313-345.

Pearson, J. R. A., 1958, "On Convection Cells Induced by Surface Tension," Journal of Fluid Mechanics, Vol. 4, pp. 489-500.

Pimputkar, S.M., and S. Ostrach, 1981, "Convection Effects In Crystal Grown From the Melt," Journal of Crystal Growth, Vol. 55, pp. 614-646.

Saunders, B.V., B.T. Murray, G.B. McFadden, S.R. Coriell, and A.A. Wheeler, 1992, "The effect of Gravity Modulation on Thermosolutal Convection in an Infinite Layer of Fluid", Physics of Fluids A, Vol. 4, No. 6.

Skarda , J.R.L., Jacqmin, D., McCaughan, F.E., "Exact and Approximate Solutions to the Double-Diffusive Marangoni-Benard Problem With Cross-Diffusive Terms," Journal of Fluid Mechanics, Accepted For Publication, 1998.

Terrones, G., and C.F. Chen, 1993, "Convective Stability of Gravity-Modulated Doubly Cross-Diffusive Fluid Layers," Journal Fluid Mechanics, Vol. 255, pp. 301-321.

Venezian, G., 1969, "Effect of Modulation On The Onset of Thermal Convection," Journal Of Fluid Mechanics, Vol. 35, part 2, pp. 243-354.

REPORT DOCUMENTATION PAGE

Form Approved
OMB No. 0704-0188

1. AGENCY USE ONLY (*Leave blank*)	2. REPORT DATE	3. REPORT TYPE AND DATES COVERED
	June 1998	Technical Memorandum

4. TITLE AND SUBTITLE

Convective Instability of a Gravity Modulated Fluid Layer With Surface Tension Variation

5. FUNDING NUMBERS

WU–962–24–00–00

6. AUTHOR(S)

J. Raymond Lee Skarda

7. PERFORMING ORGANIZATION NAME(S) AND ADDRESS(ES)

National Aeronautics and Space Administration
Lewis Research Center
Cleveland, Ohio 44135–3191

8. PERFORMING ORGANIZATION REPORT NUMBER

E–11219

9. SPONSORING/MONITORING AGENCY NAME(S) AND ADDRESS(ES)

National Aeronautics and Space Administration
Washington, DC 20546–0001

10. SPONSORING/MONITORING AGENCY REPORT NUMBER

NASA TM—1998-207941
AIAA–98–2599

11. SUPPLEMENTARY NOTES

Prepared for the 2nd Theoretical Fluid Mechanics Meeting sponsored by the American Institute of Aeronautics and Astronautics, Albuquerque, New Mexico, June 15–18, 1998. Responsible person, J. Raymond Lee Skarda, organization code 6712, (216) 433–8728.

12a. DISTRIBUTION/AVAILABILITY STATEMENT

Unclassified - Unlimited
Subject Categories:34 and 29 Distribution: Nonstandard

This publication is available from the NASA Center for AeroSpace Information, (301) 621–0390.

12b. DISTRIBUTION CODE

13. ABSTRACT ***(Maximum 200 words)***

Gravity modulation of an unbounded fluid layer with surface tension variations along its free surface is investigated. In parameter space of (wavenumber, Marangoni number) modulation has a destabilizing effect on the unmodulated neutral stability curve for large Prandtl number, Pr, and small modulation frequency, Ω, while a stabilizing effect is observed for small Pr and large Ω. As $\Omega \rightarrow$ oo, the modulated neutral stability curves approach the unmodulated neutral stability curve. At certain values of Pr and Ω multiple minima are observed and the neutral stability curves become highly distorted. Closed regions of subharmonic instability are also observed. Alternating regions of synchronous and subharmonic instability separated by very thin stable regions are observed in $(1/\Omega, g_1)$ space for the singly diffusive cases. Quasiperiodic behavior in addition to the synchronous and subharmonic responses are observed for the case of a double diffusive fluid layer. Minimum acceleration amplitudes were observed to closely correspond with a subharmonic response, $\lambda_{im} = \Omega/2$.

14. SUBJECT TERMS

Microgravity; Marangoni; Benard; Onset of convection; Gravity modulation; g-jitter; Floquet; Stability; Thermocapillary; Hydrodynamic stability

15. NUMBER OF PAGES

18

16. PRICE CODE

A03

17. SECURITY CLASSIFICATION OF REPORT	18. SECURITY CLASSIFICATION OF THIS PAGE	19. SECURITY CLASSIFICATION OF ABSTRACT	20. LIMITATION OF ABSTRACT
Unclassified	Unclassified	Unclassified	